Comparative Biochemistry and Physiology, Part B 256 (2021) 110626

Contents lists available at ScienceDirect

Comparative Biochemistry and Physiology, Part B

journal homepage: www.elsevier.com/locate/cbpb

Establishment and characterisation of single cell-derived embryonic stem cell lines from the gilthead seabream, *Sparus aurata*

A. Vergès-Castillo [a], I.A. González-Vargas [b,c], J.A. Muñoz-Cueto [a,d], Á.J. Martín-Robles [b,d,*], C. Pendon [b,e,*]

[a] Department of Biology, Faculty of Marine and Environmental Sciences, University of Cádiz, Puerto Real, Cádiz, Spain
[b] Bioquímica y Biología Molecular, Departamento de Biomedicina, Biotecnología y Salud Pública, Universidad de Cádiz, Puerto Real, Cádiz, Spain
[c] Departamento de Ciencias Naturales, Exactas y Estadística, Facultad de Ciencias, Universidad de Santiago de Cali, Cali, Colombia
[d] INMAR Research Institute, Marine Campus of International Excellence (CEIMAR), Agrifood Campus of International Excellence (ceiA3), The European University of the Seas (SEA-EU), University of Cádiz, Puerto Real, Cádiz, Spain
[e] INBIO, Facultad de Ciencias, Universidad de Cádiz, Puerto Real, Cádiz, Spain

ARTICLE INFO

Editor: Chris Moyes

Keywords:
Embryonic stem cell lines
Monoclonal cell line
pcna
In vitro studies
Sparus aurata
Embryoid bodies
Aquaculture

ABSTRACT

An important bottleneck in fish aquaculture research is the supply and maintenance of embryos, larvae, juvenile and adult specimens. In this context, cell lines represent alternative experimental models for *in vitro* studies that complement *in vivo* assays. This allows us to perform easier experimental design and sampling and avoid the sacrifice of animals. Embryonic stem (ES) cell lines have attracted increasing attention because they have the capability to proliferate indefinitely and could be differentiated into any cell type of the organism. To minimise cell heterogeneity and increase uniformity of *in vitro* studies results, in this manuscript we report the development and characterisation of two single cell-derived ES cell lines (monoclonal) from the morula stage embryos of the gilthead seabream, *Sparus aurata*, named as SAEC-A3 and SAEC-H7. Both cell lines have been passaged for over 100 times, indicating the establishment of long-term, immortalised ES cell cultures. Sequence analyses confirmed the seabream origin of the cell lines, and growth analyses evidenced their high viability and proliferating activity, particularly in culture medium supplemented with 10–15% fetal bovine serum and 22 °C. Both cell lines showed the ability to generate embryoid bodies and show different sensitivity and response to all-trans retinoic acid. The analysis of epithelial (*col1α1*) and neuronal (*sox3*) markers in differentiated cultures revealed that SAEC-A3 tended to differentiate towards epithelial-like cells whereas SAEC-H7 tended to differentiate towards neuronal-like cells. Both cell lines were efficiently transfected with pDsRed2-ER and/or pEGFP-N1 plasmids, indicating that they could represent useful biotechnological tools. Daily expression of *pcna* showed significant expression rhythms, with maximum levels of cell proliferation during the day-night transition. Currently, these cell lines are being successfully used as experimental models for the study of cellular metabolism, physiology and rhythms as well as for toxicological, pharmacological and gene expression analyses.

1. Introduction

Embryonic stem (ES) cells are derived from early embryonic developmental stages and show two defining properties: the ability of self-renewal, maintaining their undifferentiated characteristics, and cellular pluripotency (Fu, 2014; Hong et al., 2011). *In vitro* approaches using embryo-derived cell cultures have complemented *in vivo* studies in many disciplines such as biochemistry, biotechnology, immunology, developmental biology and chronobiology. They have provided information concerning cell proliferation and apoptosis, cell differentiation, cell signalling and metabolism, cytotoxicity, pharmacology and gene expression (Ilic et al., 2015; Reubinoff et al., 2000; Molino et al., 2019; Weger et al., 2017). Moreover, ES cells can contribute to the germ line after being transplanted into recipient embryos to generate chimaeras and gene-targeted organisms (Lin et al., 1992). Importantly, these ES cells allow us to replace and reduce the use of animals and refine tests to

* Corresponding authors at: Bioquímica y Biología Molecular, Departamento de Biomedicina, Biotecnología y Salud Pública, Facultad de Ciencias, Universidad de Cádiz, Puerto Real, Cádiz, Spain.
E-mail addresses: alba.verges@uca.es (A. Vergès-Castillo), munoz.cueto@uca.es (J.A. Muñoz-Cueto), agueda.jimena@uca.es (Á.J. Martín-Robles), carlos.pendon@uca.es (C. Pendon).

https://doi.org/10.1016/j.cbpb.2021.110626
Received 13 September 2020; Received in revised form 16 April 2021; Accepted 21 May 2021
Available online 25 May 2021

cause less damage and stress in living organisms (Sellick, 2011).

Since the first reported ES cell line developed in *Drosophila melanogaster* (Schneider, 1972), ES cells have been developed in many different species including mice (Evans and Kaufman, 1981; Martin, 1981), humans (Thomson, 1998; Reubinoff et al., 2000), and fish (Béjar et al., 2002; Cao et al., 2019; Collodi et al., 1992; Parameswaran et al., 2012; Parameswaran et al., 2007; Wakamatsu et al., 1994; Weger et al., 2017; Whitmore et al., 2000). When using these cell lines, cellular homogeneity has been shown to be a crucial factor for the success of *in vitro* studies and some methods such as gene-delivery or chimaera production (Kim and Eberwine, 2010; Silva et al., 2011; Young and Dean, 2015). These methods are usually cell specific, low in efficiency and viability and lack uniformity (Kim and Eberwine, 2010). In fact, new methodologies are being investigated to develop monoclonal lines (Yang et al., 2018). The use of monoclonal ES cell lines also reduces the genetic variability, inherent to the method of generating embryonic cell lines, the heterogeneity in cellular responses and allows to obtain more reliable and consistent results, thus favouring the understanding of cellular mechanisms. However, to the best of our knowledge, currently no monoclonal ES cell lines are available from marine fish, which could be of high relevance for studies in important commercial species.

Proliferating cell nuclear antigen (PCNA) is a conserved protein found in all eukaryotic species as well as in Archaea, which is required for DNA synthesis during replication (Bravo et al., 1987; Prelich et al., 1987; Tan et al., 1986). Expression levels of *pcna* are associated with proliferation or neoplastic transformation (Bravo et al., 1982; Celis et al., 1984), being the analysis of its expression used to evaluate cell proliferation (Tachibana et al., 2005).

Fishes represent the largest group of vertebrates, with around 32.000 species, 85 orders and 536 families (Nelson et al., 2016). They have a long evolutionary history and exhibit a great diversity in habitat, life span, size, shape, reproductive strategies and behaviour. In turn, Perciforms is the largest order of vertebrates and is among the most diverse orders of fishes, including many species of commercial interest. The gilthead seabream (*Sparus aurata*) is a marine perciform highly important for European aquaculture that is reared under both intensive and extensive conditions over the Mediterranean coasts. This species also represents an important model for basic and applied research on growth, reproduction, chronobiology, neuroanatomy, nutrition, stress, osmoregulation, development, genomics, ecotoxicology and pathology (Martínez-Barberá et al., 1995; Gothilf et al., 1996; González de Canales et al., 1996; Muñoz-Cueto et al., 1999; Muñoz-Cueto et al., 1998; Sarasquete et al., 1999; González-Martínez et al., 2006; Bodinier et al., 2010; Mata-Sotres et al., 2015; Pérez-Sánchez et al., 2018; Khansari et al., 2018; Pauletto et al., 2018). Supply, maintenance and handling of embryos, larvae, juvenile and adult of this species for research purposes entail important economic costs, as well as welfare and ethical issues. For this reason, the development of immortalised ES monoclonal cell lines derived from the gilthead seabream could provide experimental models for *in vitro* studies, thus accomplishing the objectives of the 3Rs strategy, *i.e.*, replacing (R1) the laboratory animals as long as adequate *in vitro* alternatives are available, reducing (R2) the number of laboratory animals to the greatest possible extent, and refining (R3) and minimizing the distress caused to them. For this purpose, in this study we have developed and characterized two single cell-derived ES cell lines from gilthead seabream (*Sparus aurata*) fertilised oocytes, called SAEC-A3 and SAEC-H7. We have characterized their growth and their potential in terms of capacity to form embryoid bodies and the ability to be differentiated and transfected. Moreover, we have analysed the evolution of cell proliferation under different photoperiods, revealing significant daily oscillations of proliferating activity that are endogenous to the cells. These ES cell lines could be used as valuable tools in a wide range of research assays, contributing to our understanding of cellular physiology and metabolism, cellular stress response, cytotoxicity, transgenesis and chronobiological synchronization to environmental cues in fish.

2. Material and methods

2.1. Establishment of Sparus aurata cell lines and routine maintenance

Gilthead seabream (*Sparus aurata*) fertilised oocytes were collected at morula stage from the fish facilities of the "Servicio Central de Investigación en Cultivos Marinos" (University of Cádiz). Fertilised eggs were properly disinfected with 70% ethanol and 4% bleach, washed with sterile, filtered seawater and then with phosphate buffer saline (PBS). Cells were pull out of the chorion by mechanical disruption using sterile 1.5 mL microcentrifuge tubes and a piston. Subsequently, a pool of cells was transferred to 12.5 cm^2 culture flasks with regular Leibovitz's L-15 growth medium (L-15, Gibco, Waltham, MA, USA) supplemented with 10% fetal bovine serum (FBS, Gibco), 1% penicillin/streptomycin (P/S, Gibco), 1% glutamine (Gibco) and NaCl 5 M (complete L-15 medium). When high confluence was reached, cells were transferred to 25 cm^2 flasks and then to 75 cm^2 flasks to expand the culture. Cells were passaged using 2 mL of 0.05% trypsin (Gibco) when 80% confluence was reached. Approximately 2.5×10^5 cells were replated in a new culture flash with fresh complete L-15 medium and 1.5×10^6 cells/mL were cryopreserved in completed L-15, 10% dimethyl sulfoxide (DMSO, VWR, Llinars del Vallès, Barcelona, Spain) and stored in liquid nitrogen. To ensure obtaining single cell-derived cell lines (monoclonal cell lines) a limited dilution was performed at passage 20 in a 96 well plate. More than 20 different clones were obtained and their growth was daily monitored in an inverted phase-contrast microscope (AE31 Motic). Two of them were selected to expand, called *Sparus aurata* embryonic cell lines A3 and H7 (SAEC-A3 and SAEC-H7, respectively). From the 96 well plate, SAEC-A3 and SAEC-H7 were gradually transferred to 24, 12 and 6 well plates and, finally, to culture flasks. They were passaged and cryopreserved as described above. All flasks were maintained at 22 °C in constant darkness and the culture medium was replaced every 3–4 days.

Animals were manipulated following the guidelines of the Animal Experimentation and Ethics Committee of the University of Cádiz (Spain), in accordance to the international ethical standards and the European Union regulation (EC Directive 86/609/EEC)..

2.2. Cell proliferating activity of seabream cell lines and molecular confirmation of the species identity

To confirm the proliferating activity and to ensure the *Sparus aurata* origin of SAEC-A3 and SAEC-H7 monoclonal ES cell lines, PCR amplified products of *proliferating cell nuclear antigen* (*pcna*, GenBank accession no. **KF857335.1**), *alpha 1 collagen 1* (*col1α1*, GenBank accession no. **DQ324363.1**), *cyclooxygenase-2* (*cox2*, GenBank accession no. **MG570172.1**) and *Sparus aurata* FAU *ubiquitin like and ribosomal protein S30 fusion* (*fau*, GenBank accession no. **XM_030404363**) were analysed and sequenced to corroborate their identity. Total RNA was extracted from cultured cells using the E.Z.N.A. Total RNA Kit I (Omega BIO-TEK, Norcross, Georgia, USA) supplementing the lysis buffer with β-mercaptoethanol (Sigma-Aldrich, St Louis, Missouri, USA) following the manufacturer instructions. Subsequently, 500 ng of total RNA were reverse transcribed into cDNA using the qScript cDNA Synthesis Kit (Quantabio, Beverly, MA, USA) in a 20 μL reaction volume. *pcna*, *cox2 and fau* specific primers were designed by using Primer3Plus software (http://www.bioinformatics.nl/cgi-bin/primer3plus/primer3plus.cgi) and *col1α1* primers were selected in accordance with Parameswaran et al., 2012 (Table 1). PCRs were performed in a MJ Mini™ Thermal Cycler (Bio-Rad, Alcobendas, Madrid, Spain) with the following conditions: denaturalization step at 95 °C for 30s, followed by 40 cycles of denaturalization at 95 °C for 5 s, annealing at 60 °C for 30s and elongation at 72 °C for 5 s. Amplified products were visualised in 1,5% agarose gel and were isolated and purified with a commercial kit (ISOLATE II PCR and Gel Kit, Bioline, London, UK) for sequencing (Stab Vida, Caparica, Portugal). Sequences were depurated and analysed by

Table 1
Sequences of primers used for the characterization of the *Sparus aurata* embryonic monoclonal cell lines, SAEC-A3 and SAEC-H7. PCR amplicon sizes (bp) are also indicated.

Name	Sequence (5′-3′)	Amplicon size (bp)
Sa_pcna_F	AGATGAATGAACCCGTCCAG	147
Sa_pcna_R	CGTGTCCCATATCAGCAATC	
Sa_col1α1_F	GAGATGGCGGTGATGTGGCGGAGTC	214
Sa_col1α1_R	GCCTGGTTTGGCTGGATGAAGAGGG	
Sa_cox2_F	GAGTACTGGAAGCCGAGCAC	192
Sa_cox2_R	GATATCACTGCCGCCTGAGT	
Sa_18S_F	CGAAAGCATTTGCCAAGAAT	102
Sa_18S_R	AGTTGGCACCGTTTATGGTC	
Sa_fau_F	GACACCCAAGGTTGACAAGCAG	149
Sa_fau_R	GGCATAGAAGCACTTAGGAGTTG	
Sa_sox3_F	CCCCAAAATGCACAACTCTG	126
Sa_sox3_R	TGCTCCTTCATGTGCATAGC	
Sa_bactin_F	TCCTGCGGAATCCATGAGA	51
Sa_bactin_R	GACGTCGCACTTCATGATGCT	

BLAST (https://blast.ncbi.nlm.nih.gov/Blast.cgi) to confirm seabream identity.

2.3. Cell viability assay

Viability assays of SAEC-A3 and SAEC-H7 were performed using Thiazolyl Blue Tetrazolium Bromide (MTT, Sigma-Aldrich) at a final concentration of 5 mg/mL. SAEC-A3 and SAEC-H7 cells were plated by duplicate in a 96 well plate at three different densities: 1×10^4, 2×10^4 and 3×10^4 cells/well. To test cellular viability, after 24, 48 and 72 h cells were incubated during 4 h with 20 μL MTT. Thereafter, medium was discarded and 100 μL of DMSO (Sigma-Aldrich) was added into each well to solubilise formazan crystals. Cells were maintained in DMSO in continuous shaking for 10 min. Absorbance at 570 nm was determined using a microplate reader (ThermoFisher Scientific, Waltham, MA, USA) and results (absorbance *vs.* time) were plotted to obtain an indirect measurement of viable cell number.

2.4. Optimization of culture conditions

To optimize cell viability under culture conditions of both cell lines, the effect of fetal bovine serum concentration and temperature on growth was analysed.

2.4.1. Fetal bovine serum (FBS) concentration and temperature effects

To establish the optimal FBS concentration and temperature conditions for the growth of SAEC-A3 and SAEC-H7, two experiments were performed where 1×10^4 cells/well in 1.0 mL were plated by triplicate in 12 well plates with complete L-15 medium. After 24 h, SAEC-A3 and SAEC-H7 were counted in a Neubauer chamber using Trypan Blue staining (Sigma-Aldrich) to determine the initial cell number (day 1). To investigate the effect of FBS concentration, after 24 h medium was replaced at 0%, 5%, 10% and 15% FBS in the remaining plates. In order to establish the best growing temperature conditions, SAEC-A3 and SAEC-H7 were maintained at three different temperatures (13 °C, 22 °C and 31 °C) until the end of the experiment. They were plated with L-15 10% FBS, as it was the minimum FBS concentration producing good growth and best counts in both cases. Subsequently, every 3 days culture medium was renewed in both experiments in order to guarantee appropriate culture conditions. Triplicates of every FBS concentration or a given temperature were counted in a Neubauer chamber using Trypan Blue staining (Sigma-Aldrich) at day 4, 7, 10 and 13.

2.4.2. Calculation of the generation time

Once the most favourable conditions for FBS concentration and temperature were established, the generation time of each cell line was established using the mathematical calculation according to Stephenson (2010): $\log (N) = \log (N_0) + Kt$, where N is the increase in cell number, N_0 is the number of cells at the beginning of the time interval, K is the growth constant calculated as the slope of the line plotting the log of the cell concentration *vs.* time and t is the time.

2.5. Analysis of the potential of SAEC-A3 and SAEC-H7 cell lines

To analyse the potential of SAEC-A3 and SAEC-H7, the formation of embryoid bodies, the effect of retinoic acid (RA) on cell differentiation and the capacity of cell lines to be transfected were analysed.

2.5.1. Formation of embryoid bodies

Embryoid bodies (EBs) formation, a characteristic usually associated with pluripotency, was assayed using 90 mm bacteriological petri dishes. Both cell lines were plated at a density of 5×10^6 cells/15 mL and, to verify the capacity to generate EBs, they were maintained under shaking with complete L-15 medium, constant temperature of 22 °C and total darkness for two weeks. Cells were observed every day with an inverted phase-contrast microscope for EBs formation. Once formed, EBs were collected and seeded in 12.5 cm^2 culture flasks to generate cell monolayers.

2.5.2. Cell differentiation

Cell differentiation capacity of SAEC-A3 and SAEC-H7 was analysed by seeding 2×10^4 cells/well in 6 well plates by triplicate. Cells were maintained in complete L-15 medium and after 24 h, medium was supplemented with different all-trans retinoic acid (RA) (Sigma-Aldrich) concentrations to induce cellular differentiation: 1, 2 and 4 μM. Cells plated with the corresponding DMSO concentrations were used as controls. Cells were maintained under the experimental treatments for ten days and medium was renewed every day. On day 10, RNA was extracted, and cDNA synthetised as described in Section 2.2. Epithelial (*col1α1*) and neuronal (*SRY-box containing protein 3*, *sox3*, GenBank accession no. **KM522783.1**) markers relative expression was analysed by RT-qPCR as specified in Section 2.7. Daily morphological changes were examined under an inverted phase-contrast microscope with 20× and/or 40× dry objectives.

2.5.3. Transfection studies

The ability of SAEC-A3 and SAEC-H7 cell lines to be transfected was assessed using pDsRed2-ER and/or pEGFP-N1 expression plasmids (ThermoFisher Scientific). For this purpose, 1×10^5 cells/well were plated in a 12 well plate by duplicate with complete L-15 medium. After 24 h, medium was replaced and cells were transfected by lipofection using VIROMER^R Yellow (Lipocalyx, Weinbergweg, Germany) with 1 μg/μL pDsRed2-ER and/or pEGFP-N1 (Clontech, CA, USA) following manufacturer's instructions. After 72 h, cells were fixed by using 4% paraformaldehyde-PBS (Sigma-Aldrich) for 10 min and samples were assembled in a glass slide using VECTASHIELD HardSet™ Antifade fluorescence mounting medium with DAPI, to preserve fluorescence (Vector laboratories, Burlingame, USA). Cells successfully transfected were observed and counted in an inverted fluorescence microscope (ApoTome2.0 Axion Observer, ZEISS, Oberkochen, Germany) to calculate transfection efficiency.

2.6. Daily variations and circadian rhythms of pcna expression

To analyse *pcna* daily variations in the *Sparus aurata* ES cell line SAEC-H7, 2.5×10^5 cells/well were seeded in 6 well plates by triplicates in complete L-15 medium. After 24 h, medium was replaced, and cells were maintained two entire days under 12 h light and 12 h darkness to ensure their synchronization. Expression of *pcna* was then analysed over 4 complete days by using two different experimental photoperiod groups: 12 h light and 12 h darkness during the four days (LDLD); and 12 h light and 12 h darkness during the first day and continuous light until the end of the experiment (LDLL). In the LDLD group and the first

day of the LDLL group, light was switched on at 9:00 h and off at 21:00 h local time. Cells were maintained under constant temperature (22 °C) during the complete experiment. Triplicates of SAEC-H7 were collected every 6 h at zeitgeber (ZT) or circadian time (CT) 0, 6, 12 and 18, and total RNA was extracted and retrotranscribed as previously described in Section 2.2. Daily *pcna* relative expression was analysed by real-time quantitative PCR (RT-qPCR), as indicated in Section 2.7.

2.7. Gene expression analysis

Real-time quantitative PCR (RT-qPCR) was used to analyse daily *pcna* relative expression, and *col1α1*, *sox3* relative expression. qPCR reactions were performed by triplicate in a CFX96 Touch Deep Well Real-Time PCR Detection System (Bio-Rad) using PerfeCTa SYBR Green SuperMix (Quantabio, Beverly, MA, USA). To optimise qPCR conditions, a temperature gradient was performed for each set of primers. Standard curves were also generated for each gene using 10-fold serial dilutions of cDNA, showing slopes close to −3.32 and efficiencies around 100%. Amplification conditions were as follows: denaturalization step at 95 °C for 30s, followed by 40 cycles of denaturalization at 95 °C for 5 s, annealing at 60 °C for 30s and elongation at 70 °C for 5 s. Non-template control and inter-run calibrator samples were used as negative and comparative controls. Melting curves were analysed to confirm amplification of a single product in each sample. mRNA relative expression was calculated by using ΔΔCt method (Livak and Schmittgen, 2001) using *β-actin* (GenBank accession no. **X89920.1**) and *18S*(GenBank accession no. AJ291668.1) as housekeeping genes for normalisation. Primers for *β-actin* were selected in accordance to Vera et al. (2013). All obtained PCR products were purified and sequenced to confirm their identity.

2.8. Statistical and rhythm analyses

Differences among means were analysed by one-way analysis of variance (ANOVA) followed by Tukey's post-hoc comparisons test. When data did not accomplish the ANOVA requirements (normality and homogeneity of variances), a non-parametric Kruskal-Wallis test was used. In all cases, significance was accepted at $p < 0.05$. Statistical analyses were performed using the StatGraphics Centurion software (Statpoint Technologies, Warrenton, VA, USA). All values shown in figures are presented as mean ± standard error of the mean (SEM).

Rhythm analyses of *pcna* relative expression were performed by the cosinor method (Nelson et al., 1979), using the software developed by Prof. A. Díez Noguera ("El Temps", University of Barcelona) and they were considered significant when $p < 0.05$.

3. Results

3.1. Establishment of Sparus aurata cell lines

A limited dilution has allowed us to successfully obtained two monoclonal embryonic cell lines derived from morula stage embryos of *Sparus aurata*. They were designated as SAEC-A3 and SAEC-H7 (*Sparus aurata* embryonic cell line A3 and H7). When cells were plated at low confluences, they were dispersed at the bottom of the culture flask, showing rounded and elongated morphologies (Fig. 1A, D). Proliferative cells in contact, rounded and polygonal in shape, generated small colonies that started covering the flask bottom surface (Fig. 1B, E) to finally reach high confluences (Fig. 1C, F). Rounded floating cells in division were appreciated in all culture growing stages (Fig. 1, white arrowheads). Currently, cells have been passaged for over 100 times with no apparent morphological changes (Supplementary Fig. S1), indicating the establishment of long-term immortalised cell cultures. SAEC-A3 and SAEC-H7 were regularly cryopreserved in complete L-15 medium and 10% DMSO and stored in liquid nitrogen. Cells thawed, resuspended in fresh complete medium and plated in new flasks were viable and showed over 90% survival rate.

3.2. Molecular identification of gilthead seabream cell lines and cell proliferating activity

In order to confirm that the cell lines derived from seabream, PCR products of *pcna*, *col1α1*, *cox2* and *fau* were sequenced and analysed by BLAST. Our results confirmed the seabream origin of all amplified products, with 100% identity observed in SAEC-A3 and SAEC-H7 cell lines (Fig. 2, Table 2).

Amplification of proliferating cell nuclear antigen (*pcna*) confirmed the proliferative activity of both cell lines (Fig. 2).

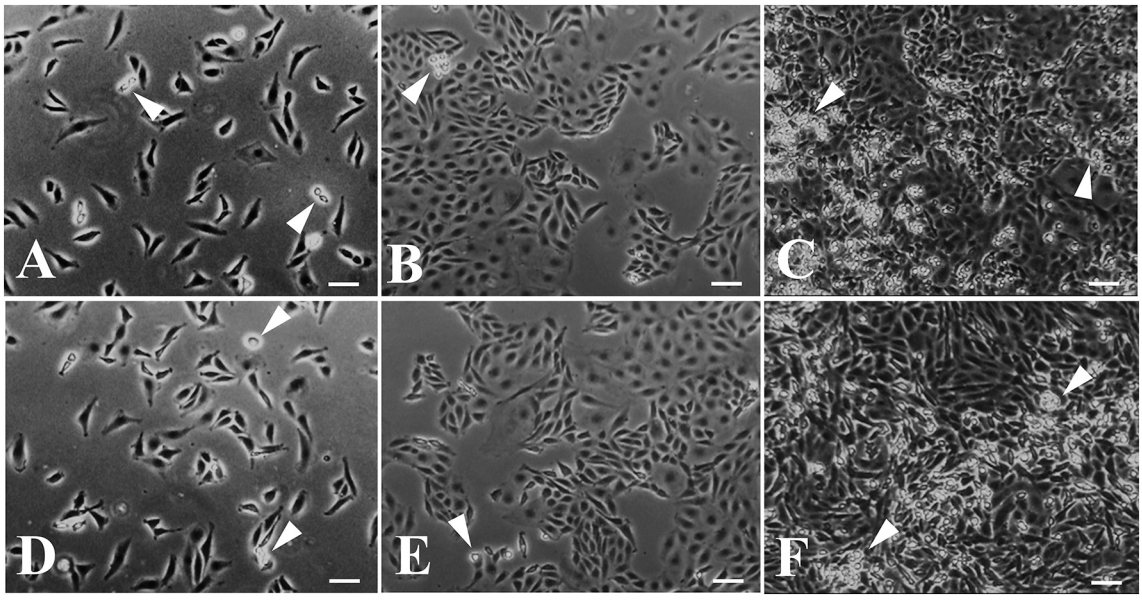

Fig. 1. Phase-contrast micrographs of growing *Sparus aurata* monoclonal cell lines SAEC-A3 (A-C) and SAEC-H7 (D—F) in culture. Individual cells showed rounded and elongated morphologies when plated at low confluences (A, D), 24 h post seeding. Small colonies are observed at medium confluences, with cells exhibiting rounded and polygonal morphology (B, E), 72 h post seeding. At high confluences, cells completely covered the bottom flask surface (C, F), more than five days in culture. White arrowheads indicate some active dividing cells. Micrographs were acquired with 20× dry objective. Scale bar: 20 μm.

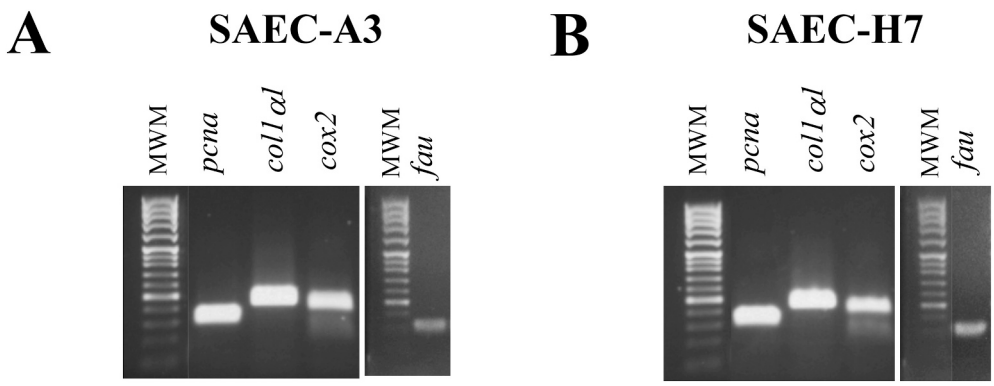

Fig. 2. Electrophoretic profile of amplicons obtained by PCR in SAEC-A3 (A) and SAEC-H7 (B) cell lines visualised in 1.5% agarose gel. *pcna*, *col1α1*, *cox2 and fau* PCR products of 147, 214, 192 and 149 bp, respectively, were amplified following the PCR conditions described in the Material and Methods section. MWM: Molecular weight marker. From bottom to top, black bars indicate 50, 100, 200 and 1000 bp.

Table 2
Sequence identity of the selected amplified products in SAEC-A3 and SAEC-H7 with the closest sequences from GenBank. Table shows accession number of each sequence in every species, E-values and percentages of query cover and identity (%). All data were collected from BLASTn.

Gene	Name of Species	Accession Number	E-value	Query cover (%)	Query identity (%)
pcna	*Sparus aurata*	XM_030418162.1	**4e-69**	100	100.00
	Acanthopagrus latus	XM_037097160.1	3e-61	98	97.24
	Seriola dumerili	XM_022766974.1	3e-60	99	96.58
	Labrus bergylta	XM_020647462.2	1e-59	98	96.55
col1α1	*Sparus aurata*	DQ324363.1	**1e-104**	100	100.00
	Acanthopagrus latus	XM_037089113.1	9e-102	100	99,06
	Cottoperca gobio	XM_029438325.1	3e-96	100	97,64
	Micropterus salmoides	XM_038692282.1	2e-93	100	96,71
cox2	*Sparus aurata*	MG570172.1	**1e-94**	100	100.00
	Acanthopagrus latus	XM_037114887.1	3e-81	98	95,85
	Pagrus major	HM453866.1	6e-78	98	94,82
	Oplegnathus fasciatus	FJ952157.3	1e-64	98	90.67
fau	*Sparus aurata*	XM_030404363.1	**3e-70**	100	100.00
	Acanthopagrus latus	XM_037087142.1	3e-65	100	97.99
	Scophthalmus maximus	XM_035617728.1	3e-61	99	96.62
	Paralichthys olivaceus	XM_020092007.1	3e-60	100	95.97

3.3. Cell viability

As expected, the best viability values were observed in higher cell confluences for both cell lines, *i.e.*, when 2×10^4 and 3×10^4 cells/well were seeded in the three different time points analysed (24, 48 and 72 h, Supplementary Fig. S2). In all densities tested, viability was higher at 72 h. Although both cell lines exhibited the same tendencies in formazan production, SAEC-H7 showed higher viability values than SAEC-A3 in the three different confluences screened (Supplementary Fig. S2).

3.4. Growth characteristics of seabream cell lines

Growth curves obtained at different serum concentrations for SAEC-A3 and SAEC-H7 indicated that both cell lines exhibited the lowest cell number when medium was devoid of FBS (0%), with no significant increase in growth over time (ANOVA *p*-value >0.05, Fig. 3). SAEC-A3 showed a steady significant rise in cell number when supplemented with 5%, 10% or 15% FBS during the first ten days (day 1, 4, 7 and 10, ANOVA *p*-values 0.00001, 0.00001 and Kruskal-Wallis p-value 0.01154 for 5%, 10% and 15% FBS, respectively). Subsequently, growth curves showed a significant decrease in proliferation at day 13 (Fig. 3A). SAEC-A3 showed the highest cellular counts when medium was supplemented with 10% and 15% FBS. However, SAEC-H7 displayed a different growth behaviour and response to FBS compared to SAEC-A3. Cells showed slower growth in low cell concentrations during the first ten days of culture with 5%, 10% and 15% FBS, showing statistically significant increments in cell number (ANOVA p-values 0.00002, 0.00806 and 0.00001, respectively). Moreover, a further significant increase in the number of viable cells was observed at day 13, indicating that after 13 days SAEC-H7 still maintained growth capacity (Fig. 3B). The highest cellular counts were also observed when medium was supplemented with 10% and 15% FBS.

Regarding temperature effects on cell growth, both cell lines showed minimum growth at 13 °C, with no significant increase in cell number in the case of SAEC-A3 (Fig. 4). Cells displayed the optimal growth at 22 °C, showing significant increments in cell number during the whole experiment with a maximum reached at day 13 (ANOVA *p*-values 0.00001 and 0.0001 for SAEC-A3 and SAEC-H7, respectively). At 31 °C, a faster growth was appreciated compared to 22 °C, and the statistical analysis showed significant increments in cell number during the first ten days of the experiment (ANOVA p-values 0.00001 for both cell lines, Fig. 4). However, the number of cells was maintained constant at day 13, tending to decrease (Fig. 4). Higher cellular counts were obtained in SAEC-H7 in relation to SAEC-A3, particularly at 31 °C (Fig. 4).

The results of viability polynomic curves analyses indicated an estimated generation time of 1.7 days for both cell lines, although the doubling time was reduced to 0.9 days during the first days (day 1, 4 and 7).

3.5. Formation of embryoid bodies

One of the defining characteristics of embryonic cells is their ability to form EBs. Both SAEC-A3 and SAEC-H7 monoclonal cell lines were able to generate EBs since the first day in continuous shaking. EBs were

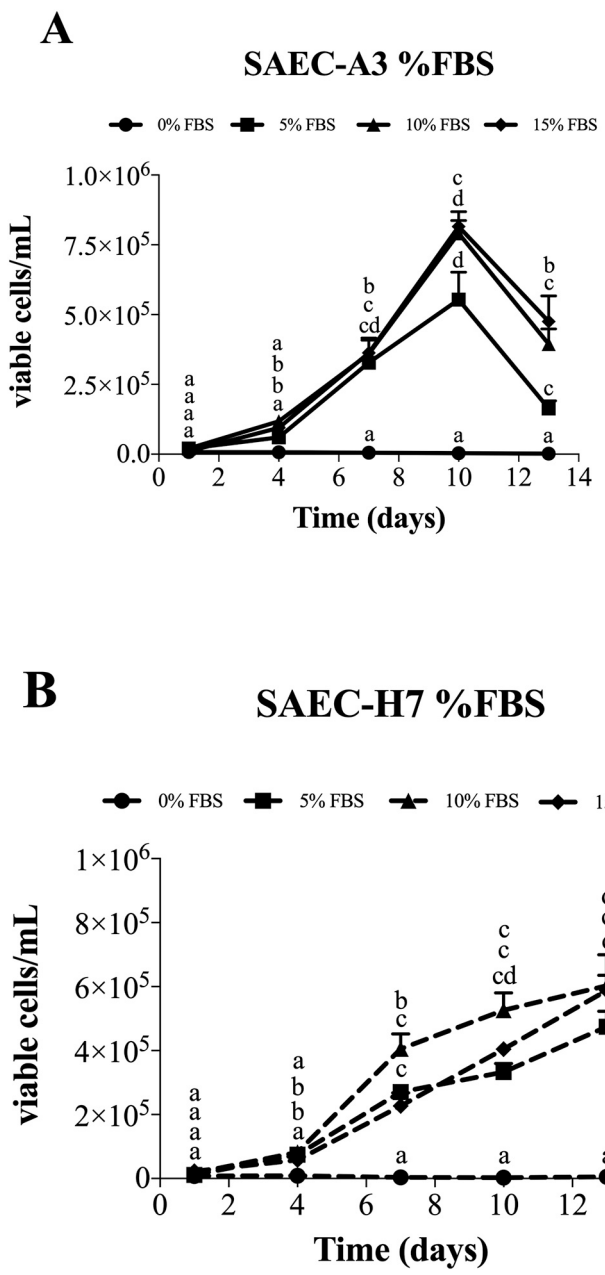

Fig. 3. Effects of fetal bovine serum (FBS) concentration on the growth of *Sparus aurata* monoclonal embryonic cell lines SAEC-A3 (A) and SAEC-H7 (B). 1×10^5 cells/mL were plated by triplicate in complete L-15 medium and constant temperature (22 °C). After 24 h, medium was supplemented with 0%, 5%, 10% and 15% FBS and cells were counted every 3 days. Curves represent viable cell number/mL. Different letters above graphs indicate significant statistical differences (ANOVA one-way $p < 0.05$). Values are represented as mean ± standard error of the mean (SEM).

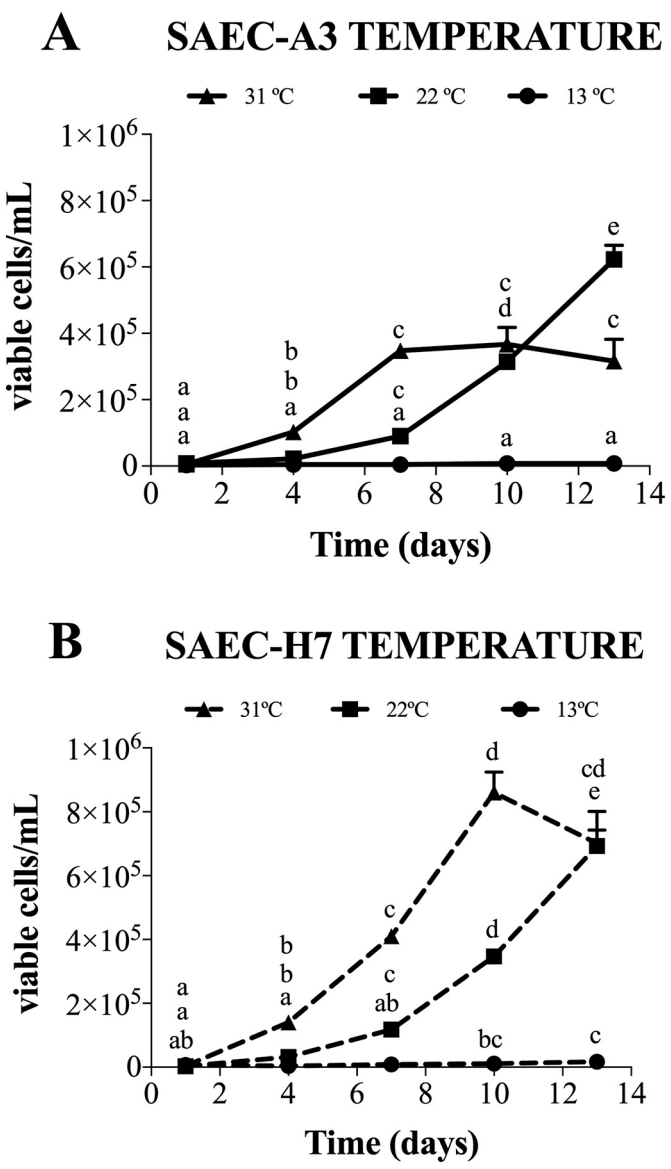

Fig. 4. Effects of temperature on the growth of *Sparus aurata* monoclonal embryonic cell lines SAEC-A3 (A) and SAEC-H7 (B). 1×10^5 cells/mL were plated by triplicate in complete L-15 medium containing 10% FBS. After 24 h, cells were maintained at three different temperatures. *i.e.*, 13 °C, 22 °C and 31 °C and were counted every 3 days. Graphs show viable cell number/mL. Different letters above graphs indicate significant statistical differences (ANOVA one-way $p < 0.05$). Values are represented as mean ± standard error of the mean (SEM).

observed as aggregate forms and were maintained during two weeks without renewing the culture medium (Fig. 5A, B). Nevertheless, daily observations showed that SAEC-A3 cells formed less EBs and needed more time than SAEC-H7 to generate them, with many single cells that remained in suspension without aggregation. After fifteen days, SAEC-A3 and SAEC-H7 EBs grew normally when they were replated in culture flasks with complete L-15 medium.

3.6. Cell differentiation

Both *Sparus aurata* cell lines responded with different sensitivity to retinoic acid (RA) treatment. In addition, our qualitative and molecular analyses highlighted different patterns of differentiation. During ten days of RA treatment, different cell types were observed in both cell lines which, by morphology, were described as neuron-like (a relatively rounded cell body with extended processes, around 7.80 ± 2,93% in SAEC-H7) (Fig. 5C, D) and epithelial-like (polygonal in shape, with expanded cytosol, stationary, growing in patches, around 3.78 ± 0.99% in SAEC-A3) cells (Fig. 5E, F), being the number of epithelial-like cells much higher in SAEC-A3. No differentiated cells were observed in control wells (Fig. 5G, H). Molecular analysis of specific epithelial (*col1α1*) and neural (*sox3*) markers revealed statistically significant differences in *col1α1* relative expression in SAEC-A3 cell line when treated with 2 and 4 μM RA concentrations (ANOVA *p*-value 0.0115 and 0.0435, respectively) (Fig. 6A). However, in SAEC-H7 monoclonal cell line, no significant differences in *col1α1* expression were observed at any

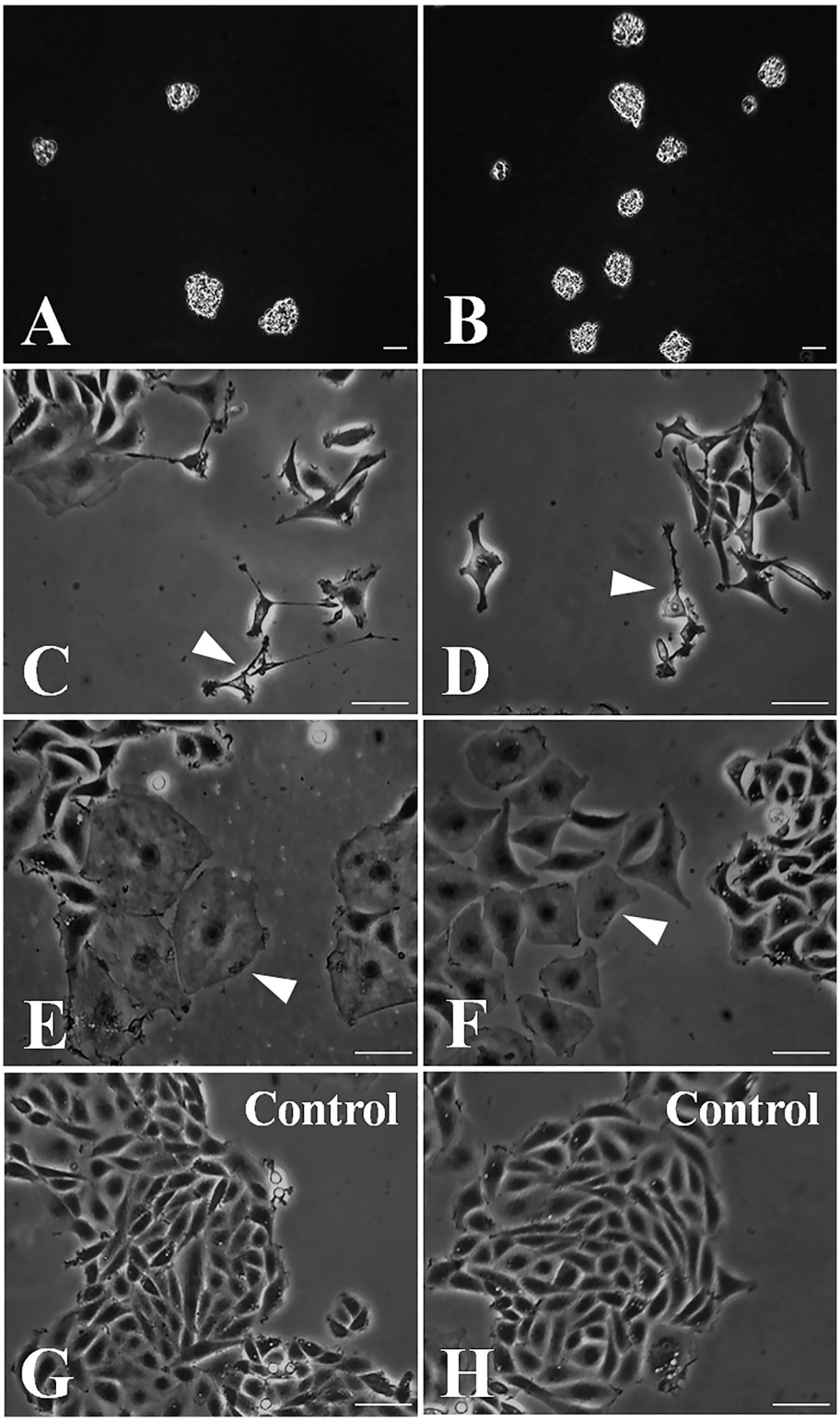

Fig. 5. Phase-contrast micrographs of embryoid bodies (EBs) formed in SAEC-A3 (A) and SAEC-H7 (B) when cells were maintained under shaking. Differentiation of SAEC-A3 (C, E, G) and SAEC-H7 (D, F, H) cells after all-trans retinoic acid treatment. White arrowheads indicate some neuron- (C, D) and epithelial-like (E, F) cells. No differentiated cells were observed in control wells (G, H). Cells were observed in an inverted phase-contrast microscope and micrographs were captured with the 40× dry objective. Scale bar: 20 μm.

RA concentration studied (data not shown). In relation to *sox3*, SAEC-A3 showed no statistically significant differences at any RA concentration studied (data not shown). On the contrary, relative expression of *sox3* in SAEC-H7 displayed statistically significant differences when cells were treated with 4 μM of RA concentrations (ANOVA p-value 0.0002) (Fig. 6B).

3.7. DsRed2-ER and EGFP-N1 transfection studies

SAEC-A3 and SAEC-H7 cell lines were successfully transfected with any or both pDsRed2-ER and/or pEGFP-N1 expression plasmids, being the estimated transformation efficiency around 1% (Fig. 7; Supplementary Fig. S3). The expression of both plasmids was detected 72 h after transfection under a fluorescence microscope. In the case of pDsRed2-ER, a cytosolic fluorescence pattern corresponding to the

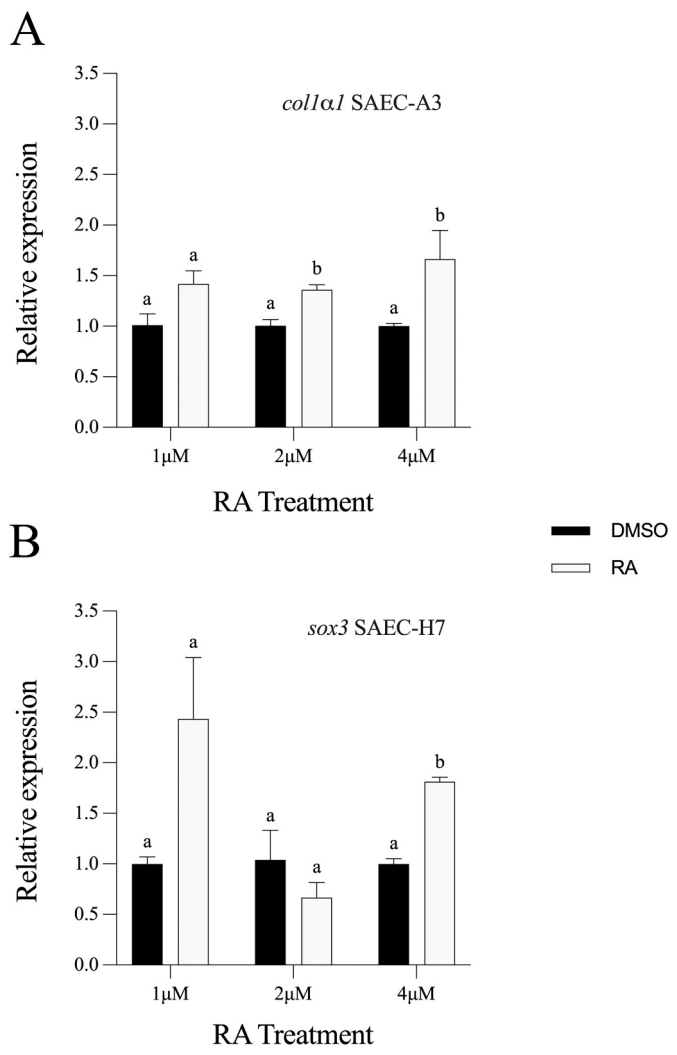

Fig. 6. Relative expression of *col1a1* in SAEC-A3 (A) and *sox3* in SAEC-H7 (B) cell lines subjected to different all-trans retinoic acid (RA) concentrations (1, 2 and 4 μM). Triplicates were collected after ten days of RA treatment and mRNA relative expression was analysed by RT-qPCR. Black bars indicate relative expression values in DMSO-control wells and white bars represent expression values in RA-treated cells. Different letters above bars indicate statistically significant differences (ANOVA p-value <0.05).

endoplasmic reticulum was observed, being more intense in the perinuclear region (Fig. 7A, E). A diffuse fluorescence in the cytosol and intense in the nucleus corresponded to pEGFP-N1 expression (Fig. 7C, G).

3.8. Daily variations and circadian rhythms of pcna expression

Daily variations and circadian rhythms in the expression of the proliferating cell nuclear antigen (*pcna*) were analysed in SAEC-H7 ES cells maintained under two different photoperiod regimes, LDLD and LDLL (Fig. 8).

When SAEC-H7 cells were maintained under 12 h light and 12 h darkness (LDLD) during 4 consecutive days, *pcna* relative expression

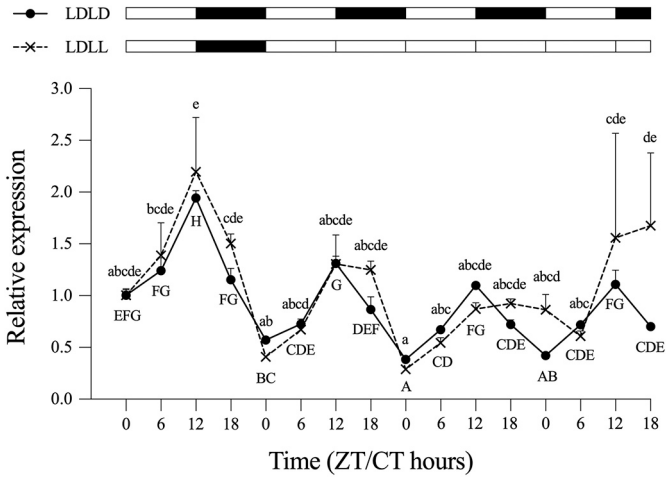

Fig. 8. Daily variations in relative expression of *pcna* in SAEC-H7 cells maintained under two different photoperiods regimes (LDLD and LDLL). Triplicates were collected every 6 h during 4 complete days and mRNA relative expression was analysed by RT-qPCR. Time in hours in the x-axis represent zeitgeber time in LD conditions (ZT) and circadian time in LL conditions (CT). Capital letters along the graph show the statistical differences for the LDLD group and the lower-case letters indicate the statistical differences for the LDLL groups. The bars above the graph indicate daily photoperiod conditions. White bars represent the light phase (ZT0 to ZT12 in LDLD; ZT0 to ZT12 for the first day and ZT0 to ZT18 for the last three days in LDLL) and black bars represent the dark phase (ZT12 to ZT0 in LDLD; ZT12 to ZT0 for the first day in LDLL). Different letters indicate statistically significant differences between mean values (p-value < 0.05).

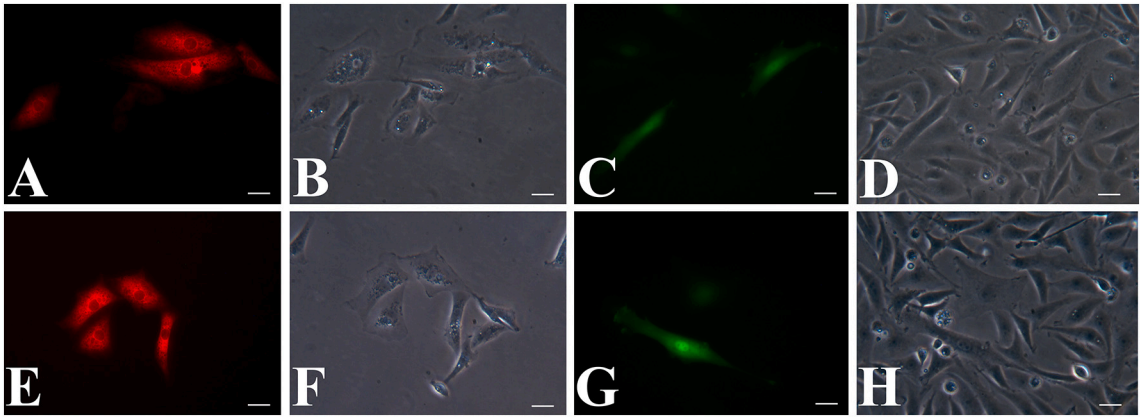

Fig. 7. Fluorescence micrographs of SAEC-A3 (A-D) and SAEC-H7 (*E*-H) cells transfected with pDsRed2-ER (A and E) or pEGFP-N1 (C and G) expression plasmids using VIROMER Yellow transfection reagent. Micrographs of the corresponding bright-field images are also shown (B, F, D, H). Cells were observed in an inverted fluorescence microscope and micrographs were captured with the 40× dry objective. Scale bar: 20 μm. (For interpretation of the references to colour in this figure legend, the reader is referred to the web version of this article.)

Table 3
Parameters defining *pcna* gene expression rhythms in SAEC-H7 ES cell line when maintained under two different photoperiods for 4 days:12 h light 12 h darkness (**LDLD**) and 12 h light 12 h darkness during the first day and constant light until the end (**LDLL**). Numeric values of mesor, amplitude, acrophase and significance of the rhythm (*p*-value) reported by the cosinor analysis are indicated. Mesor and amplitude are given as relative expression values (r.e.) and acrophase as zeitgeber (ZT)/circadian time (CT). Rhythms were considered significant when $p < 0.05$. Significance: $*p < 0.05$, $**p < 0.01$, $***p < 0.001$, $****p < 0.0001$. N.S. non-significant rhythms.

pcna	Mesor (r.e.)	Amplitude (r.e.)	Acrophase (ZT/CT)	Significance (*p*-value)
LDLD				
Day 1	1.33	0.47	11.64	**
Day 2	0.86	0.37	12.71	***
Day 3	0.71	0.35	12.28	****
Day 4	0.73	0.34	11.88	***
LDLL				
Day 1	1.51	0.58	12.38	*
Day 2	0.90	0.53	14.18	**
Day 3	0.65	0.35	13.98	***
Day 4	1.17	0.63	15.79	N.S.

showed statistically significant differences in all days analysed (ANOVA *p*-value 0.00001), with peaks of expression at ZT12 and lower levels at ZT0 (Fig. 8). Cosinor analysis revealed that *pcna* exhibited significant daily rhythms of expression during the four days analysed, with acrophases at the day-night transition (from ZT11.64 to 12.71), mesors ranging from 0.71 to 1.33 and amplitudes ranging from 0.34 to 0.47 (Table 3).

Under LDLL conditions, *pcna* transcript levels in SAEC-H7 showed a similar daily profile than that observed for LDLD conditions (ANOVA p-value 0.002360, Fig. 8), but statistical differences were restricted to the first day (between ZT12-ZT18 and ZT0) and the fourth day analysed (between CT6 and CT18, Fig. 8). Cosinor analysis showed significant rhythms during the first three days, indicating the existence of a circadian rhythm in *pcna* transcript levels (Table 3). During the first day, *pcna* acrophase was placed during the day-night transition at ZT12.38. Subsequently, acrophases were delayed in the next following days under constant light and placed at CT14.18 and CT13.98. Declining mesor values and amplitudes were observed, ranging from 1.51 to 0.90 and 0.65 and from 0.58 to 0.53 and 0.35, respectively (Table 3). During the fourth day under LDLL conditions the rhythm in *pcna* expression was lost (Fig. 8).

4. Discussion

In this work, we have established two single cell-derived ES cell lines, designated as SAEC-A3 and SAEC-H7, from gilthead seabream, *Sparus aurata*, an important commercial fish species. To the best of our knowledge, these are the only available monoclonal cell lines derived from a marine fish species at the moment. We have determined the optimal conditions for their culture and maintenance as well as described their principal characteristics and potentials and their daily proliferating activity. Cells showed high viability under different culture conditions, were able to form embryoid bodies and to be successfully differentiated and transfected, making them suitable alternative models to complement *in vivo* studies in this species.

A limited dilution was performed to isolate individual cells that were expanded to obtain monoclonal cell lines, avoiding genetic diversity and cellular heterogeneity. Limiting-dilution procedures in cell line development have been widely used to generate single cell-derived cell lines (Wurm, 2004). Maximisation of cellular homogeneity by developing single cell-derived cell lines could represent a key factor for the success of *in vitro* studies, gene-delivery methods or chimaera formation, which are often cell-specific and low in efficiency when applicable to a population of cells that lack uniformity (Kim and Eberwine, 2010; Silva et al., 2011; Yang et al., 2018; Young and Dean, 2015). In this context, SAEC-A3 and SAEC-H7 are glimpsed as powerful systems to explore the multiple applications of the genetic manipulation.

Both cell lines were derived from morula stage embryos and displayed all distinctive features of ES-like cells (Evans and Kaufman, 1981; Martin, 1981). These included a typical ES phenotype with small size and rounded/polygonal shape without prolongations or signs of primary tissue organization, stable growth forming compacted cell colonies capable of expansion, and the ability to differentiate into several cell types (Béjar et al., 2002; Collodi et al., 1992; Hong et al., 2011; Hong et al., 1996; Parameswaran et al., 2012; Parameswaran et al., 2007). Furthermore, SAEC-A3 and SAEC-H7 cells showed the ability to spontaneously form embryoid bodies when grown in suspension, a characteristic of ES cells associated with pluripotency that constitutes an important initial step in directed differentiation (Brickman and Serup, 2017; Martin and Evans, 1975). At present, cells have been passaged for over 100 times, exhibiting continuous growth in culture for over 3 years without evident changes in their morphology, providing evidence for their ability of self-renewal and their undifferentiated state. SAEC-A3 and SAEC-H7 cells were maintained in conventional Leibovitz's 15 medium supplemented with 10% FBS at 22 °C in constant darkness, similar to other marine fish cells reported to date (Béjar et al., 2002; Buonocore et al., 2006; Gignac et al., 2014; Molino et al., 2019; Olivares-Ferretti et al., 2019; Parameswaran et al., 2012; Parameswaran et al., 2007; Servili et al., 2009). Altogether, these facts indicate the establishment of two viable cell populations, each derived from one cell that can be considered immortalised, permanent ES cell lines with self-renewal and differentiation capabilities, and suitable for early vertebrate development assays (Collodi et al., 1992; Ghosh and Collodi, 1994).

The growth of SAEC-A3 and SAEC-H7 was characterized in different assays, showing the capability to adapt to different temperatures (13-31 °C) and FBS concentrations (5–15%). A supplementation of 10% FBS and 22 °C were observed to be the most appropriate conditions for the growth of seabream ES cells. This temperature is within the optimal temperature range for embryonic development of *Sparus aurata*, that has been reported to be 16–22 °C (Polo et al., 1991). Additionally, our results indicated that the lower temperature (13 °C) is not suitable for maintaining a continuous growth of seabream cells, especially SAEC-A3. Accordingly, low temperatures have also been revealed as critical for *Sparus aurata* aquaculture in the Mediterranean during winter. Cooling below 18 °C initiated cellular stress responses in several tissues and temperatures under 14 °C reduced the metabolic rate in this species, compromising the rates of growth and reproduction (Kyprianou et al., 2010). These results supported that SAEC-A3 and SAEC-H7 can be maintained under different environmental conditions, suggesting that they could be used as a tool for experimental *in vitro* assays to test biotic (*e.g.* feeding) and abiotic (*e.g.* temperature) factors in this species. These growth curves showed the usual profile of *in vitro* cultures (Stephenson, 2010) and doubling times (1.7 days) were similar to those reported for other fish embryonic cell lines (Béjar et al., 2002; Buonocore et al., 2006; Moon et al., 2006; Yuan et al., 2013). Furthermore, viability and growth curves results suggest that cells could be used as a model for cytotoxic studies (Fotakis and Timbrell, 2006; Molino et al., 2019; Vega et al., 2017), tissue regeneration (Gonzalez Gonzalez et al., 2018) or tumoural investigation (Gil-Benso et al., 2017).

One way to assess pluripotency in ES cell lines is to determine the ability to form embryoid bodies (EBs) (Brickman and Serup, 2017). Both SAEC-A3 and SAEC-H7 were able to generate EBs under shaking.

Formation of EBs in ES cell lines was first described by Martin and Evans (Martin and Evans, 1975). Since that moment, many researches evidenced the importance of EBs differentiation as an experimental model to shed light on early embryonic development (Desbaillets et al., 2000; Höpfl et al., 2004; Livigni et al., 2009; Parameswaran et al., 2012; Thomson, 1998). In fact, not all cell cultures have the attribute to generate EBs, and only ES cells that are immortal, long-term cell cultures and derived from blastocyst stages have been shown to exhibit it (Brickman and Serup, 2017). Therefore, EBs formation from *Sparus aurata* ES cell lines A3 and H7 confirmed the pluripotency of both embryonic cell lines. This has also been demonstrated in mammalian ES cells (Robertson, 1987) and other ES cell lines developed from fish (Fan and Collodi, 2006; Ghosh and Collodi, 1994; Hong et al., 1996; Li et al., 2019).

Another important criteria for evaluation of pluripotency is the potential to differentiate into distinct cell lineages (Brickman and Serup, 2017; Evans and Kaufman, 1981; Martin, 1981). Embryonic stem cells could produce skin cells, neurons, melanocytes, muscle cells, blood cells and even gametes to generate structured and complex tissues and organisms (Ikeda et al., 2018; Ito et al., 2010; Lehtonen et al., 1989; Schwartz et al., 2008). In this sense, ES cells are potent research tools because they could open new possibilities to produce different cell types. In fact, this technique has been used in many species, including humans and non-human primates (Thomson, 1998; Peura et al., 2007), as well as fish species (Fan and Collodi, 2006; Gignac et al., 2014; Molino et al., 2019; Parameswaran et al., 2012; Parameswaran et al., 2007; Wang et al., 2011). Our results showed the ability of SAEC-A3 and SAEC-H7 cells to undergo differentiation in response to all-trans retinoic acid, thus further supporting their pluripotency. SAEC-A3 and SAEC-H7 showed different sensitivity to retinoic acid, which reinforces the different individuality of each of the lines obtained. Differentiated cells were described by morphology as neuron- and epithelial-like cells. Both qualitative (morphology observation) and quantitative (molecular) results suggested slightly different patterns of differentiation, where SAEC-A3 showed a tendency to differentiate to epithelial cells and SAEC-H7 to neuronal cells. Similar observations have been described in mammals and other fish ES cell lines (Chen et al., 2015; Hong et al., 1996; Kuai et al., 2009; Nakano et al., 1994; Peura et al., 2007; Wakamatsu et al., 1994; Wang et al., 2011). Altogether, our results support the embryonic and pluripotent nature of SAEC-A3 and SAEC-H7 cell lines, reinforcing their appropriateness as *in vitro* models for the study of extracellular factors influencing cell differentiation and to delve into the early development of *Sparus aurata* and other fish species.

In the present study, we also showed that both monoclonal ES cell lines could be transfected with plasmids, pDsRed2-ER and/or pEGFP-N1, using liposomes. They were functional in the expression of genes transfected. Fluorescence patterns were representative of patterns previously described in human breast cancer cells (Figueroa et al., 2017), mouse cell lines (Decembrini et al., 2017) or cell lines derived from freshwater fish species like medaka, *Oryzias latipes*, and zebrafish, *Danio rerio* (Malo et al., 2017; Yokota et al., 2016). The possibility to introduce DNA into these cell lines allows their suitability to be used as models to analyse the regulation of gene expression and as a platform to produce recombinant proteins, as well as for methods of genetic manipulation, thus allowing chimaera formation, genetic modifications in transgenic animals or gene knockout techniques in fish (Parameswaran et al., 2012; Schmöhl et al., 2019; Turner et al., 2018; Yokota et al., 2016).

The daily proliferative activity of these cells was analysed by measuring *pcna* expression in SAEC H7. *pcna* expression profile exhibited daily variations and significant rhythms under light-dark photoperiods, with maximum levels at the day-night transition. Maintenance of these rhythms under constant light conditions suggests the involvement of a circadian clock in driving them. This phenomenon has been previously described in zebrafish larvae and cell cultures (Dekens et al., 2003) and in the retina of *Haplochromis burtoni* (Chiu et al., 1995). From single-cell organisms to humans, circadian clock-generated synchronization of an organism's cell division cycle with environmental factors could represent a key strategic adaptation, placing an important event at the most appropriate time to ensure its survival and success (Johnson, 2010; Bernard and Herzel, 2006). By restricting cell division events at the end of the day or at night, the clock would help to avoid UV-induced DNA damage in cell division and in developing animals (*e.g.*, fish floating eggs, embryos and larvae) or to suppress potential tumor growth in adult animals (Bernard and Herzel, 2006; Johnson, 2010; Shostak, 2017). Therefore, a better understanding of the mechanisms linking the cell cycle and the circadian clock in these embryonic stem cells could contribute to enlarge our knowledge of this connection and to optimise many rhythmic physiological processes affecting the aquaculture and wellbeing of seabream and other species.

5. Conclusions

In the present work, we have generated and characterized two monoclonal embryonic cell lines derived from gilthead seabream, named SAEC-A3 and SAEC-H7. Each line showed different sensitivity to all-trans retinoic acid and a tendency to differentiate into different cell types. We have also shown that SAEC-H7 showed a variable and rhythmic daily profile in *pcna* expression and therefore in proliferative activity. In conclusion, our results highlight the versatility of both *Sparus aurata* single cell-derived ES cell lines, SAEC-A3 and SAEC-H7, to be applicable as a new experimental model for *in vitro* assays in an economically important species such as the gilthead seabream. The availability of such monoclonal cell lines could increase reliability of *in vitro* studies results and make possible new approaches to the study of early embryonic development and differentiation, cellular metabolism, cytotoxicity, environmental synchronization, gene expression and its regulation and functional genomics. Additionally, this tool could permit us to replace the use of animals wherever possible in research assays, to reduce the number of animals used and to refine tests to cause animals the minimum distress, thus accomplishing the 3R's rule.

Supplementary data to this article can be found online at https://doi.org/10.1016/j.cbpb.2021.110626.

Declaration of Competing Interest

The authors declare that they have no known competing financial interests or personal relationships that could have appeared to influence the work reported in this paper.

Acknowledgments

This work was funded by grants from the Spanish Ministry of Science, Innovation and Universities (AGL2017-82582-C3-1-R, AGL2013-49027-C3-2-R) to JAMC. AVC is a FPI fellow (PRE2018-085642) funded by the Spanish Ministry of Science, Innovation and Universities.

References

Béjar, J., Hong, Y., Alvarez, M.C., 2002. An ES-like cell line from the marine fish Sparus aurata: characterization and chimaera production. Transgenic Res. 11, 279–289. https://doi.org/10.1023/A:1015678416921.

Bernard, S., Herzel, H., 2006. Why do cells cycle with a 24 hour period? Genome Inform 17, 72–79. https://doi.org/10.11234/gi1990.17.72.

Bodinier, C., Sucré, E., Lecurieux-Belfond, L., Blondeau-Bidet, E., Charmantier, G., 2010. Ontogeny of osmoregulation and salinity tolerance in the gilthead sea bream *Sparus aurata*. Comp. Biochem. Physiol. A Mol. Integr. Physiol. 157, 220–228. https://doi.org/10.1016/j.cbpa.2010.06.185.

Bravo, R., Fey, S.J., Bellatin, J., Larsen, P.M., Celis, J.E., 1982. Identification of nuclear polypeptide ('cyclin') whose relative proportion is sensitive to changes in the rate of cell proliferation and to transformation. Prog. Clin. Biol. Res. 85 (part A), 235–248.

Bravo, R., Frank, R., Blundell, P.A., Macdonald-Bravo, H., 1987. Cyclin/PCNA is the auxiliary protein of DNA polymerase-delta. Nature 326, 515–517.

Brickman, J.M., Serup, P., 2017. Properties of embryoid bodies. Wiley Interdiscip. Rev. Dev. Biol. 6, 1–11. https://doi.org/10.1002/wdev.259.

Buonocore, F., Libertini, A., Prugnoli, D., Mazzini, M., Scapigliati, G., 2006. Production and characterization of a continuous embryonic cell line from sea bass (*Dicentrarchus labrax* L.). Mar. Biotechnol. 8, 80–85. https://doi.org/10.1007/s10126-005-5032-2.

Cao, Z., Mao, X., Luo, L., 2019. Germline stem cells drive ovary rgeneration in zebrafish. Cell Rep. 26, 1709–1717.e3. https://doi.org/10.1016/j.celrep.2019.01.061.

Celis, J.E., Bravo, R., Larsen, P.M., Fey, S.J., 1984. Cyclin: a nuclear protein whose level correlates directly with the proliferative state of normal as well as transformed cells. Leuk. Res. 8, 143–157.

Chen, T., Wang, F., Wu, M., Wang, Z.Z., 2015. Development of hematopoietic stem and progenitor cells from human pluripotent stem cells. J. Cell. Biochem. 116 (7), 1179–1189. https://doi.org/10.1002/jcb.25097.

Chiu, J.F., Mark, A.F., Fernald, R.D., 1995. Daily rhythms of cell proliferation in the teleost retina. Brain Res. 673, 119–125.

Collodi, P., Kame, Y., Ernst, T., Miranda, C., Buhler, D.R., Barnes, D.W., 1992. Culture of cells from zebrafish (*Brachydanio rerio*) embryo and adult tissues. Cell Biol. Toxicol. 8, 43–61. https://doi.org/10.1007/BF00119294.

Decembrini, S., Martin, C., Sennlaub, F., Chemtob, S., Biel, M., Samardzija, M., Moulin, A., Behar-Cohen, F., Arsenijevic, Y., 2017. Cone genesis tracing by the Chrnb4-EGFP mouse line: evidences of cellular material fusion after cone precursor transplantation. Mol. Ther. 25, 634–653. https://doi.org/10.1016/j.ymthe.2016.12.015.

Dekens, M.P.S., Santoriello, C., Vallone, D., Grassi, G., Whitmore, D., Foulkes, N.S., 2003. Light regulates the cell cycle in Zebrafish. Curr. Biol. 13, 2051–2057. https://doi.org/10.1016/j.cub.2003.10.022.

Desbaillets, I., Ziegler, U., Groscurth, P., Gassmann, M., 2000. Embryoid bodies: an in vitro model of mouse embryogenesis. Exp. Physiol. 85, 645–651. https://doi.org/10.1111/j.1469-445X.2000.02104.x.

Evans, M.J., Kaufman, M.H., 1981. Establishment in culture of pluripotential cells from mouse embryos. Nature. 292, 154–156. https://doi.org/10.1038/292154a0.

Fan, L., Collodi, P., 2006. Zebrafish embryonic stem cells. Methods Enzymol. 418, 64–77. https://doi.org/10.1016/S0076-6879(06)18004-0.

Figueroa, E., Bugga, P., Asthana, V., Chen, A.L., Stephen Yan, J., Evans, E.R., Drezek, R. A., 2017. A mechanistic investigation exploring the differential transfection efficiencies between the easy-to-transfect SK-BR3 and difficult-to-transfect CT26 cell lines. J. Nanobiotechnol. 15, 1–15. https://doi.org/10.1186/s12951-017-0271-8.

Fotakis, G., Timbrell, J.A., 2006. In vitro cytotoxicity assays: comparison of LDH, neutral red, MTT and protein assay in hepatoma cell lines following exposure to cadmium chloride. Toxicol. Lett. 160 (2), 171–177. https://doi.org/10.1016/j.toxlet.2005.07.001.

Fu, X., 2014. The immunogenicity of cells derived from induced pluripotent stem cells. Cell. Mol. Immunol. 11, 14–16. https://doi.org/10.1038/cmi.2013.60.

Ghosh, C., Collodi, P., 1994. Culture of cells from zebrafish (*Brachydanio rerio*) blastula-stage embryos. Cytotechnology. 14, 21–26. https://doi.org/10.1007/BF00772192.

Gignac, S.J., Vo, N.T.K., Mikhaeil, M.S., Alexander, J.A.N., MacLatchy, D.L., Schulte, P. M., Lee, L.E.J., 2014. Derivation of a continuous myogenic cell culture from an embryo of common killifish, *Fundulus heteroclitus*. Comp. Biochem. Physiol. A Mol. Integr. Physiol. 175, 15–27. https://doi.org/10.1016/j.cbpa.2014.05.002.

Gil-Benso, R., Megías, J., San-Miguel, T., Pinto, S., Callaghan, R.C., López-Ginés, C., Cerdá-Nicolás, M., 2017. Characterization of the new human pleomorphic undifferentiated sarcoma TP53-null cell line mfh-val2. Cytotechnology. 69, 539–550. https://doi.org/10.1007/s10616-017-0112-5.

González de Canales, M.L., Muñoz-Cueto, J.A., Arellano, J., García-García, A., Sarasquete, C., 1996. Histological and histochemical characteristics of the lymphocystis disease in gilthead seabream, *Sparus aurata* L. from the south-atlantic coast of Spain. Eur. J. Histochem. 40, 143–152. 8839709.

Gonzalez Gonzalez, M., Cichon, I., Scislowska-Czarnecka, A., Kolaczkowska, E., 2018. Challenges in 3D culturing of neutrophils: assessment of cell viability. J. Immunol. Methods 457, 73–77. https://doi.org/10.1016/j.jim.2018.02.015.

González-Martínez, D., Sarasquete, C., Pascual, E., Muñoz-Cueto, J.A., 2006. Expression of gonadotrophin-releasing hormone binding sites in somatic tissues of the gilthead seabream (*Sparus aurata*): a quantitative autoradiographic study. Histol. Histopathol. 21, 1065–1073. https://doi.org/10.14670/HH-21.1065.

Gothilf, Y., Muñoz-Cueto, J.A., Sagrillo, C.A., Selmanoff, M., Chen, T.T., Kah, O., Elizur, A., Zohar, Y., 1996. Three forms of gonadotropin-releasing hormone in a perciform fish (*Sparus aurata*): complementary deoxyribonucleic acid characterization and brain localization. Biol. Reprod. 55, 636–645. https://doi.org/10.1095/biolreprod55.3.636.

Hong, Y., Winkler, C., Schartl, M., 1996. Pluripotency and differentiation of embryonic stem cell lines from the medakafish (*Oryzias latipes*). Mech. Dev. 60, 33–44. https://doi.org/10.1016/S0925-4773(96)00596-5.

Hong, N., Li, Z., Hong, Y., 2011. Fish stem cell cultures. Int. J. Biol. Sci. 7, 392–402. https://doi.org/10.7150/ijbs.7.392.

Höpfl, G., Gassmann, M., Desbaillets, I., 2004. Differentiating embryonic stem cells into Embryoid bodies. In: Schatten, H. (Ed.), Germ Cell Protocols. Methods in Molecular BiologyTM, 254. Humana Press, pp. 79–98. https://doi.org/10.1385/1-59259-741-6:079 (ISBN: 978-1-59259-741-3).

Ikeda, K., Kawasaki, Y., Matsuda, H., Kishida, S., Iwasaki, A., Ohata, S., Urashima, Y., Hirotani, Y., 2018. Approach for differentiating trophoblast cell lineage from human induced pluripotent stem cells with retinoic acid in the absence of bone morphogenetic protein 4. Placenta. 71, 24–30. https://doi.org/10.1016/J.PLACENTA.2018.10.001.

Ilic, D., Devito, L., Miere, C., Codognotto, S., 2015. Human embryonic and induced pluripotent stem cells in clinical trials. Br. Med. Bull. 116, 19–27. https://doi.org/10.1093/bmb/ldv045.

Ito, Y., Tanaka, H., Okamoto, H., Ohshima, T., 2010. Characterization of neural stem cells and their progeny in the adult zebrafish optic tectum. Dev. Biol. 342, 26–38. https://doi.org/10.1016/j.ydbio.2010.03.008.

Johnson, C.H., 2010. Circadian clocks and cell division: What's the pacemaker? Cell Cycle 9, 3864–3873. https://doi.org/10.4161/cc.9.19.13205.

Khansari, A.R., Balasch, J.C., Vallejos-Vidal, E., Parra, D., Reyes-López, F.E., Tort, L., 2018. Comparative immune- and stress-related transcript response induced by air exposure and *Vibrio anguillarum* bacterin in rainbow trout (*Oncorhynchus mykiss*) and gilthead seabream (*Sparus aurata*) mucosal surfaces. Front. Immunol. 9, 856. https://doi.org/10.3389/fimmu.2018.00856.

Kim, T.K., Eberwine, J.H., 2010. Mammalian cell transfection: the present and the future. Anal. Bioanal. Chem. 397, 3173–3178. https://doi.org/10.1007/s00216-010-3821-6.

Kuai, X.L., Gagliardi, C., Flaat, M., Bunnell, B.A., 2009. Differentiation of nonhuman primate embryonic stem cells along neural lineages. Differentiation. 77, 229–238. https://doi.org/10.1016/j.diff.2008.10.014.

Kyprianou, T.D., Pörtner, H.O., Anestis, A., Kostoglou, B., Feidantsis, K., Michaelidis, B., 2010. Metabolic and molecular stress responses of gilthead seam bream *Sparus aurata* during exposure to low ambient temperature: an analysis of mechanisms underlying the winter syndrome. J. Comp. Physiol. B. 180, 1005–1018. https://doi.org/10.1007/s00360-010-0481-y.

Lehtonen, E., Laasonen, A., Tienari, J., 1989. Teratocarcinoma stem cells as a model for differentiation in the mouse embryo. Int. J. Dev. Biol. 33, 105–115. https://doi.org/10.1387/ijdb.2485690.

Li, J., Jia, P., Chen, X., Lai, M., Jin, F., Liu, W., Yi, M., Jia, K., 2019. Establishment and characterization of a fin tissue cell line derived from silver pomfret, v. J. Fish Dis. 42, 1391–1399. https://doi.org/10.1111/jfd.13059.

Lin, S., Long, W., Chen, J., Hopkins, N., 1992. Production of germ-line chimeras in zebrafish by cell trasplants from genetically pigmented to albino embryos. Proc. Natl. Acad. Sci. U. S. A. 89, 4519–4523. https://doi.org/10.1073/pnas.89.10.4519.

Livak, K.J., Schmittgen, T.D., 2001. Analysis of relative gene expression data using real-time quantitative PCR and the 2(-Delta Delta C(T)) method. Methods 25, 402–408. https://doi.org/10.1006/meth.2001.1262.

Livigni, A., Villegas, A.N., Oikonomopoulou, I., Rahman, A., Morrison, G.M., Brickman, J.M., 2009. Differentiation of embryonic stem cells into anterior definitive endoderm. Curr. Protoc. Stem Cell Biol. 10, 1G.3.1–1G.3.10. https://doi.org/10.1002/9780470151808.sc01g03s10.

Malo, M.C., Duchemin, A.L., Guglielmi, L., Patzel, E., Sel, S., Auffarth, G.U., Carl, M., Poggi, L., 2017. The zebrafish anillin-eGFP reporter marks late dividing retinal precursors and stem cells entering neuronal lineages. PLoS One 12, 1–15. https://doi.org/10.1371/journal.pone.0170356.

Martin, G.R., 1981. Isolation of a pluripotent cell line from early mouse embryos cultured in medium conditioned by teratocarcinoma stem cells. Proc. Natl. Acad. Sci. U. S. A. 78, 7634–7638. https://doi.org/10.1073/pnas.78.12.7634.

Martin, G.R., Evans, M.J., 1975. Differentiation of clonal teratocarcinoma cells: formation of embryoid bodies in vitro. Proc. Natl. Acad. Sci. U. S. A. 72, 1441–1445. https://doi.org/10.1073/pnas.72.4.1441.

Martínez-Barberá, J.P., Pendón, C., Martí-Palanca, H., Calduch-Giner, J.A., Rodríguez, R. B., Valdivia, M.M., Pérez-Sánchez, J., 1995. The use of recombinant gilthead sea bream (*Sparus aurata*) growth hormone for radioiodination and standard preparation in radioimmunoassay. Comp. Biochem. Physiol. A Physiol. 110, 335–340. https://doi.org/10.1016/0300-9629(94)00178-v.

Mata-Sotres, J.A., Martínez-Rodríguez, G., Pérez-Sánchez, J., Sánchez-Vázquez, F.J., Yúfera, M., 2015. Daily rhythms of clock gene expression and feeding behavior during the larval development in gilthead seabream, *Sparus aurata*. Chronobiol. Int. 32, 1061–1074. https://doi.org/10.3109/07420528.2015.1058271.

Molino, C., Filippi, S., Stoppiello, G.A., Meschini, R., Angeletti, D., 2019. In vitro evaluation of cytotoxic and genotoxic effects of Di(2-ethylhexyl)-phthalate (DEHP) on European sea bass (*Dicentrarchus labrax*) embryonic cell line. Toxicol. in Vitro 56, 118–125. https://doi.org/10.1016/j.tiv.2019.01.017.

Moon, S.Y., Park, Y. Bin, Kim, D.S., Oh, S.K., Kim, D.W., 2006. Generation, culture, and differentiation of human embryonic stem cells for therapeutic applications. Mol. Ther. 13, 5–14. https://doi.org/10.1016/j.ymthe.2005.09.008.

Muñoz-Cueto, J.A., Sarasquete, C., Kah, O., 1998. The torus longitudinalis in the gilthead seabream: an undescribed fiber tract link with the valvula cerebelli. Histol. Histopathol. 13, 391–394. https://doi.org/10.14670/HH-13.391.

Muñoz-Cueto, J.A., Burzawa-Gérard, E., Kah, O., Valotaire, Y., Pakdel, F., 1999. Cloning and sequencing of the gilthead sea bream estrogen receptor cDNA. DNA Seq. 10, 75–84. https://doi.org/10.3109/10425179909008421.

Nakano, T., Kodama, H., Honjo, T., 1994. Generation of lymphohematopoietic cells from embryonic stem cells in culture. Science. 265, 1098–1101. https://doi.org/10.1126/science.8066449.

Nelson, W., Tong, Y.L., Lee, J.K., Halberg, F., 1979. Methods for cosinor-rhythmometry. Chronobiologia 6, 305–323.

Nelson, J.S., Grande, T.C., Wilson, M.V.H., 2016. Fishes of the World, 5th edition. John Wiley & Sons, Hoboken, New Jersey (ISBN: 978-1-118-34233-6).

Olivares-Ferretti, P., Hernandez, K., Peredo-Parada, M., Chavez, V., Carmona, E., Astuya, A., Parodi, J., 2019. Polyphenols obtained from *Didymosphenia geminata* (Lyngbye) Schmith altered the viability and proliferation of salmonids cells lines SHK-1 and CHSE-214. Aquat. Toxicol. 211, 141–147. https://doi.org/10.1016/j.aquatox.2019.03.022.

Parameswaran, V., Shukla, R., Bhonde, R., Hameed, A.S.S., 2007. Development of a pluripotent ES-like cell line from Asian sea bass (*Lates calcarifer*) - an oviparous stem cell line mimicking viviparous ES cells. Mar. Biotechnol. 9, 766–775. https://doi.org/10.1007/s10126-007-9028-y.

Parameswaran, V., Laizé, V., Gavaia, P.J., Leonor Cancela, M., 2012. ESSA1 embryonic stem like cells from gilthead seabream: a new tool to study mesenchymal cell lineage differentiation in fish. Differentiation. 84, 240–251. https://doi.org/10.1016/j.diff.2012.07.004.

Pauletto, M., Manousaki, T., Ferraresso, S., Babbucci, M., Tsakogiannis, A., Louro, B., Vitulo, N., Quoc, V.H., Carraro, R., Bertotto, D., Franch, R., Maroso, F., Aslam, M.L., Sonesson, A.K., Simionati, B., Malacrida, G., Cestaro, A., Caberlotto, S., Sarropoulou, E., Mylonas, C.C., Power, D.M., Patarnello, T., Canario, A.V.M., Tsigenopoulos, C., Bargelloni, L., 2018. Genomic analysis of *Sparus aurata* reveals the evolutionary dynamics of sex-biased genes in a sequential hermaphrodite fish. Commun. Biol. 1, 119. https://doi.org/10.1038/s42003-018-0122-7.

Pérez-Sánchez, J., Simó-Mirabet, P., Naya-Català, F., Martos-Sitcha, J.A., Perera, E., Bermejo-Nogales, A., Benedito-Palos, L., Calduch-Giner, J.A., 2018. Somatotropic axis regulation unravels the differential effects of nutritional and environmental factors in growth performance of marine farmed fishes. Front. Endocrinol. (Lausanne) 9, 687. https://doi.org/10.3389/fendo.2018.00687.

Peura, T., Bosman, A., Stojonov, T., 2007. Derivation of human embryonic stem cell lines. Theriogenology 67, 32–42. https://doi.org/10.1016/j.theriogenology.2006.09.031.

Polo, A., Yúfera, M., Pascual, E., 1991. Effects of temperature on egg and larval development of *Sparus aurata* L. Aquaculture 92, 367–375. https://doi.org/10.1016/0044-8486(91)90042-6.

Prelich, G., Tan, C.K., Kostura, M., Mathews, M.B., So, A.G., Downey, K.M., Stillman, B., 1987. Functional identity of proliferating cell nuclear antigen and a DNA polymerase-delta auxiliary protein. Nature 326, 517–520.

Reubinoff, B.E., Pera, M.F., Fong, C.Y., Trounson, A., Bongso, A., 2000. Embryonic stem cell lines from human blastocysts: somatic differentiation in vitro. Nat. Biotechnol. 18, 399–404. https://doi.org/10.1038/74447.

Robertson, E.J., 1987. Embryo-derived stem cell lines. In: Robertson, E.J. (Ed.), Teratocarcinomas and Embryonic Stem Cells: A Practical Approach. IRL Press, Oxford, pp. 71–112.

Sarasquete, C., Muñoz-Cueto, J.A., Ortiz, J.B., Rodríguez-Gómez, F.J., Dinis, M.T., Segner, H., 1999. Immunocytochemical distribution of cytochrome P4501A (CYP1A) in developing gilthead seabream, *Sparus aurata*. Histol. Histopathol. 14, 407–415. https://doi.org/10.14670/HH-14.407.

Schmöhl, F., Peters, V., Schmitt, C.P., Poschet, G., Büttner, M., Li, X., Weigand, T., Poth, T., Volk, N., Morgenstern, J., Fleming, T., Nawroth, P.P., Kroll, J., 2019. CNDP1 knockout in zebrafish alters the amino acid metabolism, restrains weight gain, but does not protect from diabetic complications. Cell. Mol. Life Sci. 76, 4551–4568. https://doi.org/10.1007/s00018-019-03127-z.

Schneider, I., 1972. Cell lines derived from late embryonic stages of *Drosophila melanogaster*. J. Embryol. Exp. Morpholog. 27, 353–365. 4625067.

Schwartz, P.H., Brick, D.J., Stover, A.E., Loring, J.F., Müller, F.J., 2008. Differentiation of neural lineage cells from human pluripotent stem cells. Methods 45, 142–158. https://doi.org/10.1016/j.ymeth.2008.03.007.

Sellick, J., 2011. Enhancing the protection of animals used for scientific purposes. Environ. Law Manag. 23, 75–82.

Servili, A., Bufalino, M.R., Nishikawa, R., de Melo, I.S., Muñoz-Cueto, J.A., Lee, L.E.J., 2009. Establishment of long term cultures of neural stem cells from adult sea bass, *Dicentrarchus labrax*. Comp. Biochem. Physiol. A Mol. Integr. Physiol. 152, 245–254. https://doi.org/10.1016/j.cbpa.2008.10.018.

Shostak, A., 2017. Circadian clock, cell division, and cancer: from molecules to organism. Int. J. Mol. Sci. 18, 873. https://doi.org/10.3390/ijms18040873.

Silva, G., Poirot, L., Galetto, R., Smith, J., Montoya, G., Duchateau, P., Paques, F., 2011. Meganucleases and other tools for targeted genome engineering: perspectives and challenges for gene therapy. Curr. Gene Ther. 11, 11–27. https://doi.org/10.2174/156652311794520111.

Stephenson, F.H., 2010. Calculation for molecular biology and biotechnology. In: A Guide to Mathematics in the Laboratory, 2nd ed. Academic Press, p. 2010 (ISBN: 0123756901).

Tachibana, K.E., Gonzalez, M.A., Nicholas Coleman, N., 2005. Cell-cycle-dependent regulation of DNA replication and its relevance to cancer pathology. J. Pathol. 205 (2), 123–129. https://doi.org/10.1002/path.1708.

Tan, C.K., Castillo, C., So, A.G., Downey, K.M., 1986. An auxiliary protein for DNA polymerase-delta from fetal calf thymus. J. Biol. Chem. 261, 12310–12316.

Thomson, J.A., 1998. Embryonic stem cell lines derived from human blastocysts. Science. 282, 1145–1147. https://doi.org/10.1126/science.282.5391.1145.

Turner, A.N., Andersen, R.S., Bookout, I.E., Brashear, L.N., Davis, J.C., Gahan, D.M., Gotham, J.P., Hijaz, B.A., Kaushik, A.S., Mcgill, J.B., Miller, V.L., Moseley, Z.P., Nowell, C.L., Patel, R.K., Rodgers, M.C., Shihab, Y.A., Walker, A.P., Glover, S.R., Foster, S.D., Challa, A.K., 2018. Analysis of novel domain-specific mutations in the zebrafish ndr2/cyclops gene generated using CRISPR-Cas9 RNPs. J. Genet. 97, 1315–1325. https://doi.org/10.1007/s12041-018-1033-6.

Vega, F.M., Gautier, V., Fernandez-Ponce, C.M., Extremera, M.J., Altelaar, A.F.M., Millan, J., Tellez, J.C., Hernandez-Campos, J.A., Conejero, R., Bolivar, J., Pardal, R., Garcia-Cózar, F.J., Aguado, E., Heck, A.J.R., Duran-Ruiz, M.C., 2017. The atheroma plaque secretome stimulates the mobilization of endothelial progenitor cells ex vivo. J. Mol. Cell. Cardiol. 105, 12–23. https://doi.org/10.1016/j.yjmcc.2017.02.001.

Vera, L.M., Negrini, P., Zagatti, C., Frigato, E., Sánchez-Vázquez, F.J., Bertolucci, C., 2013. Light and feeding entrainment of the molecular circadian clock in a marine teleost (*Sparusaurata*). Chronobiol. Int. 30 (5), 649–661. https://doi.org/10.3109/07420528.2013.775143.

Wakamatsu, Y., Ozato, K., Sasado, T., 1994. Establishment of a pluripotent cell line derived from a medaka (*Oryzias latipes*) blastula embryo. Mol. Mar. Biol. Biotechnol. 3, 185–191. 8000476.

Wang, D., Manali, D., Wang, T., Bhat, N., Hong, N., Li, Z., Wang, L., Yan, Y., Liu, R., Hong, Y., 2011. Identification of pluripotency genes in the fish medaka. Int. J. Biol. Sci. 7, 440–451. https://doi.org/10.7150/ijbs.7.440.

Weger, M., Diotel, N., Dorsemans, A.C., Dickmeis, T., Weger, B.D., 2017. Stem cells and the circadian clock. Dev. Biol. 431, 111–123. https://doi.org/10.1016/j.ydbio.2017.09.012.

Whitmore, D., Foulkes, N.S., Sassone-Cosi, P., 2000. Light acts directly on organs and cells in culture to set the vertebrate circadian clock. Nature. 404, 87–91. https://doi.org/10.1038/35003589.

Wurm, F.M., 2004. Production of recombinant protein therapeutics in cultivated mammalian cells. Nat. Biotechnol. 22, 1393–1398. https://doi.org/10.1038/nbt1026.

Yang, R., Lemaître, V., Huang, C., Haddadi, A., McNaughton, R., Espinosa, H.D., 2018. Monoclonal cell line generation and CRISPR/Cas9 manipulation via single-cell electroporation. Small 14, e1702495. https://doi.org/10.1002/smll.201702495.

Yokota, S., Matsuno, R., Kato, H., Hashimoto, H., Kinoshita, M., Yokoi, H., Suzuki, T., 2016. Establishment of oct4:egfp transgenic and oct4:egfp /β-actin:DsRed double transgenic medaka lines. In Vitro Cell. Dev. Biol. Anim. 52, 646–653. https://doi.org/10.1007/s11626-016-0020-6.

Young, L.J., Dean, D.A., 2015. Eletroporation mediated gene delivery. Physiol. Behav. 176, 100–106. https://doi.org/10.1016/j.gde.2016.03.011.

Yuan, Y., Huang, X., Zhang, L., Zhu, Y., Huang, Y., Qin, Q., Hong, Y., 2013. Medaka haploid embryonic stem cells are susceptible to Singapore grouper iridovirus as well as to other viruses of aquaculture fish species. J. Gen. Virol. 94, 2352–2359. https://doi.org/10.1099/vir.0.054460-0.